

on NK-susceptible populations. In this respect, it is important to determine whether peptide variability exists within the T11 molecule.

Although the recent finding of a third T-cell-specific cDNA clone encoding a putative nonglycosylated T-cell receptor-like molecule, termed  $\gamma$ , suggested that the  $\gamma$  gene and its product may be operational in T3<sup>-</sup>T11<sup>+</sup> NK populations as a receptor (19), this possibility has been excluded by transcriptional analysis. No  $\gamma$  mRNA sequences were detected in two T3<sup>-</sup>T11<sup>+</sup> clones examined.

JEROME RITZ

THOMAS J. CAMPEN

REINHOLD E. SCHMIDT

HANS DIETER ROYER

THIERRY HERCEND\*

REBECCA E. HUSSEY

ELLIS L. REINHERZ

Division of Tumor Immunology,  
Dana-Farber Cancer Institute, and  
Departments of Medicine and  
Pathology, Harvard Medical School,  
Boston, Massachusetts 02115

#### References and Notes

1. R. B. Herberman and J. R. Ortaldo, *Science* **214**, 24 (1981); G. Trinchieri and B. Perussia, *Lab. Invest.* **50**, 489 (1984).
2. T. Timonen, J. R. Ortaldo, R. B. Herberman, *J. Exp. Med.* **153**, 569 (1981).
3. T. Hercend et al., *J. Immunol.* **129**, 1299 (1982); T. Hercend et al., *Nature (London)* **301**, 158 (1983); R. E. Schmidt et al., *J. Immunol.*, in press; G. Dennert, G. Yogeewaran, S. Yamagata, *J. Exp. Med.* **153**, 545 (1981); J. F. Warner and G. Dennert, *Nature (London)* **300**, 31 (1982); P. Allavena and J. R. Ortaldo, *J. Immunol.* **132**, 2363 (1984).
4. Y. Chien et al., *Nature (London)* **312**, 31 (1984); M. Fabbi et al., *ibid.*, p. 269; C. H. Hannum et al., *ibid.*, p. 65; H. Saito et al., *ibid.*, p. 36; G. Siu et al., *ibid.* **311**, 344 (1984).
5. O. Acuto et al., *Proc. Natl. Acad. Sci. U.S.A.* **81**, 3851 (1984); N. Gascoigne et al., *Nature (London)* **310**, 387 (1984); S. M. Hedrick et al., *ibid.* **308**, 149 (1984); G. Siu et al., *Cell* **37**, 393 (1984); Y. Yanagi et al., *Nature (London)* **308**, 145 (1984); Y. Yoshikai et al., *ibid.* **312**, 521 (1984); P. E. Barker et al., *Science* **226**, 348 (1984).
6. J. R. Ortaldo et al., *J. Immunol.* **127**, 2401 (1981); B. Perussia et al., *ibid.* **130**, 2133 (1983); L. L. Lanier et al., *ibid.* **131**, 1789 (1981); T. Hercend et al., *J. Clin. Invest.*, in press.
7. S. C. Meuer et al., *Science* **218**, 471 (1982).
8. T. Hercend et al., *J. Exp. Med.* **158**, 1547 (1983); S. C. Meuer et al., *Science* **222**, 1239 (1983).
9. T. Hercend et al., *Eur. J. Immunol.* **14**, 844 (1984).
10. J. W. Goding and A. W. Harris, *Proc. Natl. Acad. Sci. U.S.A.* **78**, 4530 (1981).
11. O. Acuto et al., *Cell* **34**, 717 (1983).
12. H. D. Royer et al., *ibid.* **39**, 261 (1984).
13. H. D. Royer et al., *Proc. Natl. Acad. Sci. U.S.A.*, in press.
14. O. Acuto et al., *J. Exp. Med.*, in press.
15. F. Alt et al., *EMBO J.* **3**, 1209 (1984).
16. D. A. Fox et al., *J. Immunol.* **134**, 330 (1985).
17. R. E. Schmidt et al., *ibid.*, in press.
18. S. C. Meuer et al., *Cell* **36**, 897 (1984).
19. H. Saito et al., *Nature (London)* **309**, 757 (1984); D. M. Krantz et al., *ibid.* **313**, 752 (1985); D. Raulet et al., *ibid.* **314**, 103 (1985).
20. A. P. Feinberg and B. Vogelstein, *Anal. Biochem.* **132**, 6 (1983).
21. Supported in part by NIH grants CA 34183, AI 19807, and AI 21226. J.R. is a scholar of the Leukemia Society of America; T.C. is a fellow of the Leukemia Society of America; R.S. is a recipient of a fellowship (Schm 596/1-1) from the Deutsche Forschungsgemeinschaft; T.H. is a special fellow of the Leukemia Society of America.

\* Present address: Cellular Biology Unit, Institut Gustave-Roussy, Villejuif, France.

## Imaging Elemental Distribution and Ion Transport in Cultured Cells with Ion Microscopy

**Abstract.** Both elemental distribution and ion transport in cultured cells have been imaged by ion microscopy. Morphological and chemical information was obtained with a spatial resolution of approximately 0.5  $\mu\text{m}$  for sodium, potassium, calcium, and magnesium in freeze-fixed, cryofractured, and freeze-dried normal rat kidney cells and Chinese hamster ovary cells. Ion transport was successfully demonstrated by imaging  $\text{Na}^+$ - $\text{K}^+$  fluxes after the inhibition of  $\text{Na}^+$ - and  $\text{K}^+$ -dependent adenosine triphosphatase with ouabain. This method allows measurements of elemental (isotopic) distribution to be related to cell morphology, thereby providing the means for studying ion distribution and ion transport under different physiological, pathological, and toxicological conditions in cell culture systems.

Most cells expend much of their energy in maintaining ionic balance, and ions play an important role in intracellular regulatory events. Cells grown in cultures provide an excellent model for studying the distribution and transport of ions under normal and pathological conditions. Ion microscopy, a technique that provides visual ion images with cell morphology, is ideally suited for such studies.

Ion microscopy is based on secondary ion mass spectrometry (SIMS), and the details of the technique have been reported (1, 2). In brief, the sample to be analyzed is mounted on a conducting substrate (silicon wafers or tantalum disks, for example) and placed in the high-vacuum ( $10^{-7}$  to  $10^{-8}$  torr) sample chamber of the ion microscope. The sample is then bombarded with a primary ion beam ( $\text{O}_2^+$ ,  $\text{Ar}^+$ , and so forth), which removes the top two or three atomic layers of the sample surface by sputtering. A fraction of these atoms leave the surface as ions. These sput-

tered secondary ions are then accelerated into a double-focusing mass spectrometer that separates them according to their mass-to-charge ratio. The ion optics of the instrument preserves the spatial distribution of the emitted secondary ions through the mass spectrometer so that a one-to-one correspondence is maintained between the position of a sputtered ion leaving the sample surface and its position in the final mass-resolved ion image. This final magnified ion image reveals the spatial distribution of any selected element (in both free and bonded states) within an area up to 400  $\mu\text{m}$  in diameter with a spatial resolution of  $\sim 0.5 \mu\text{m}$ . A micro-channelplate detector, coupled with a fluorescent screen, converts the ion image into a visible image. The visible ion images produced in this fashion can be recorded directly from the fluorescent screen of the ion microscope with a 35-mm camera. Because multielement distributions can be evaluated from the same cells in this way, we have been able to image the

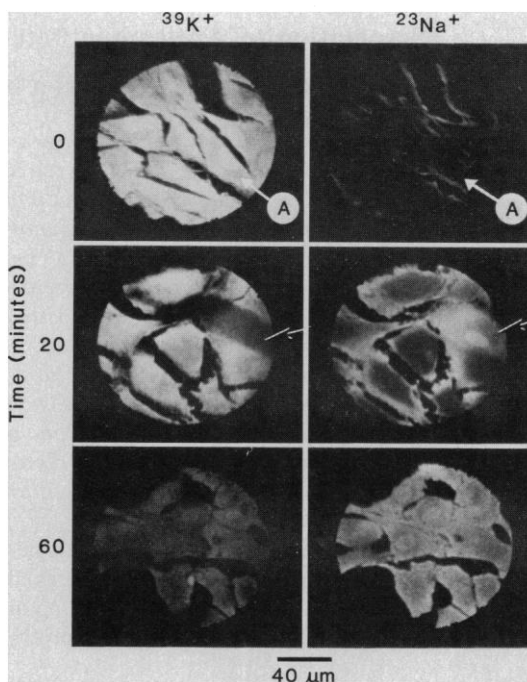


Fig. 1. Imaging  $\text{Na}^+$ - $\text{K}^+$  ion transport in NRK cells after inhibition of the  $\text{Na}^+$ - and  $\text{K}^+$ -dependent adenosine triphosphatase of the plasma membrane with a specific inhibitor, ouabain. Time (in minutes) indicates the exposure of cells to ouabain. The ion images of potassium ( $^{39}\text{K}^+$ ) are in the left column and the corresponding sodium ( $^{23}\text{Na}^+$ ) images are on the right for each treatment. At 0 minutes, the arrow marked A indicates the same cell. Brightness indicates relative ion intensities. A dead cell with high sodium and very low potassium is indicated by the arrow in the images made after 20 minutes of treatment with ouabain.

intracellular distribution and the transport of physiologically important ions in cultured cells using cryotechniques.

Semiconductor-grade silicon wafers (General Diode) were used as the substrate for cell growth, since an electrical conducting sample mount is a requirement for ion-microscopic analysis. This substrate is nontoxic and provides cell growth rates and morphologies comparable to those of cells grown on glass cover slips. Dulbecco's modified Eagle's medium with 10 percent calf serum (Gibco) was used for cell growth. Normal rat kidney (NRK) cells were seeded at a density of  $3.0 \times 10^5$  to  $3.5 \times 10^5$  cells per 100-mm plastic dish (Falcon) and incubated at 37°C in a 5 percent CO<sub>2</sub> atmosphere. Each petri dish contained approximately ten silicon wafers (3). The cells were treated with ouabain in about 4 days, when they had reached confluency. Ouabain (1 mM; Sigma) was used to inhibit the Na<sup>+</sup>- and K<sup>+</sup>-dependent adenosine triphosphatase of the plasma membrane. The samples were collected after 0, 20, and 60 minutes of treatment with ouabain. In preparation for ion-microscopic analysis, these samples were freeze-fixed with liquid nitrogen slush (-206°C), cryofractured under liquid nitrogen by a sandwich technique (4), and freeze-dried at -80°C for 24 hours. An ion microscope (Cameca model IMS-3f) operating with an 8.0-KeV O<sub>2</sub><sup>+</sup> primary ion beam and monitoring positive secondary ions was used for this study (5). When the Na<sup>+</sup>-K<sup>+</sup> ion transport was imaged as a function of time, all instrumental parameters (primary beam density, energy slits, channelplate gain, and so on), image exposure times (1 second), and photographic processing times were kept constant between treatments.

The intracellular distribution of sodium and potassium and Na<sup>+</sup>-K<sup>+</sup> ion transport in NRK cells are shown in Fig. 1. At 0 minutes after treatment with ouabain, high potassium and low sodium intensities were observed, for example, as seen in cell A. Within each cell, the intensity of potassium was slightly higher in the nucleus than in the cytoplasm.

Cells sampled after 20 minutes and 60 minutes of ouabain treatment showed an intracellular increase in sodium and loss of potassium with time (Fig. 1). These observations have been confirmed with Chinese hamster ovary cells and 3T3 cells.

Ion images showing cell morphology can be produced for any element (or isotope) of interest. In addition to sodium and potassium, other physiologically important elements such as calcium, magnesium, chloride, and phosphorus

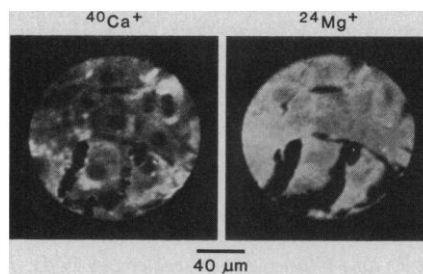


Fig. 2. The ion images of <sup>40</sup>Ca<sup>+</sup> (left) and <sup>24</sup>Mg<sup>+</sup> (right), illustrating the intracellular distribution of calcium and magnesium in freeze-fractured NRK cells.

can also be studied. The distribution of calcium and magnesium in NRK cells as revealed by ion micrographs (Fig. 2) showed that calcium concentrates more in the cytoplasm than in the nuclei of the cells. Even within the cytoplasm calcium is not homogeneously distributed, whereas the distribution of magnesium is almost homogeneous throughout the cell. The intracellular distribution of calcium is markedly different from that of sodium, potassium, and magnesium. This observation has been confirmed in several cell lines. It is known that calcium-binding organelles, such as mitochondria and the endoplasmic reticulum, and calcium-binding proteins are present in the cytoplasm.

The exposure time to produce the images in Fig. 2 was 30 seconds, and the calcium image was recorded first. The longer exposure times were required because of the low intracellular concentrations of these elements. Even after 10 minutes of ion bombardment, no noticeable preferential etching was observed

between the nuclei and the cytoplasm of the fractured cells.

The ion microscope is capable of detecting all elements (isotopes) from hydrogen to uranium with sensitivities in the parts-per-million range.

Our results show that ion microscopy, applied to cell culture systems, can be a useful method for studying ion distribution and ion transport under different physiological, pathological, and toxicological conditions.

SUBHASH CHANDRA  
GEORGE H. MORRISON

Baker Laboratory of Chemistry,  
Cornell University,  
Ithaca, New York 14853

#### References and Notes

1. R. Castaing and G. Slodzian, *J. Microsc. (Paris)* **1**, 395 (1962).
2. G. H. Morrison and G. Slodzian, *Anal. Chem.* **47** (No. 11), 932A (1975).
3. The silicon wafers (approximately 1 cm<sup>2</sup>) were washed in deionized distilled water and sterilized before they were seeded with cells. Cells were grown on the polished surface to allow visual examination with a reflected light microscope. The rough sides of the wafers were numbered to identify different treatments.
4. The details of this sandwich technique were presented at the 1984 Annual Conference of the American Society for Cell Biology [S. Chandra *et al.*, *J. Cell Biol.* **99** (No. 4), part 2, 424a (1984).], and a manuscript is in preparation. This technique makes it possible to fracture cells without removing them from the substrate. In addition, it eliminates the need for washing the extracellular nutrient media and cryosectioning before ion microanalysis. Only the fractured cells are used for ion microanalysis.
5. A mass-filtered, 400-nA O<sub>2</sub><sup>+</sup> primary ion beam (diameter, 100 μm) was directed onto a 250 by 250 μm<sup>2</sup> raster. The secondary ions were extracted from a circular region (diameter, 150 μm) centered within the raster.
6. We thank E. Racker for reviews of the ouabain experiment and the manuscript and C. Coulter and the Cornell biophysics facility for culturing cells. Supported by grant R01GM24314 from the National Institutes of Health.

25 January 1985; accepted 5 April 1985

## Dissociation of Antitumor Potency from Anthracycline Cardiotoxicity in a Doxorubicin Analog

**Abstract.** *The search for new congeners of the leading anticancer drug doxorubicin has led to an analog that is approximately 1000 times more potent, noncardiotoxic at therapeutic dose levels, and non-cross-resistant with doxorubicin. The new anthracycline, 3'-deamino-3'-(3-cyano-4-morpholinyl)doxorubicin (MRA-CN), is produced by incorporation of the 3' amino group of doxorubicin in a new cyanomorpholinyl ring. The marked increase in potency was observed against human ovarian and breast carcinomas in vitro; it was not accompanied by an increase in cardiotoxicity in fetal mouse heart cultures. Doxorubicin and MRA-CN both produced typical cardiac ultrastructural and biochemical changes, but at equimolar concentrations. In addition, MRA-CN was not cross-resistant with doxorubicin in a variant of the human sarcoma cell line MES-SA selected for resistance to doxorubicin. Thus antitumor efficacy was dissociated from both cardiotoxicity and cross-resistance by this modification of anthracycline structure.*

The anthracycline doxorubicin has become one of the most important drugs in the treatment of human cancers (1). In addition to toxicity against normal proliferating tissues, such as the bone marrow and gastrointestinal tract, anthracyclines are associated with cardiac damage related to both the total dose and the sched-

erating tissues, such as the bone marrow and gastrointestinal tract, anthracyclines are associated with cardiac damage related to both the total dose and the sched-